CPC(HEP & NP), 2009, **33**(2): 127—134 Chinese Physics C Vol. 33, No. 2, Feb., 2009

Nonlinear optimization of the modern synchrotron radiation storage ring based on frequency map analysis*

TIAN Shun-Qiang(田顺强)[1,2;1)] LIU Gui-Min(刘桂民)[1;2)] LI Hao-Hu(李浩虎)[1]
HOU Jie(后接)[1,2] CHEN Guang-Ling(陈光玲)[1,2] WAN Cheng-Lan(万承兰)[1,2]

1 (Shanghai Institute of Applied Physics, Chinese Academy of Sciences, Shanghai 201800, China)
2 (Graduate University of Chinese Academy of Sciences, Beijing 100049, China)

Abstract In this paper, we present a rule to improve the nonlinear solution with frequency map analysis (FMA), and without frequently revisiting the optimization algorithm. Two aspects of FMA are emphasized. The first one is the tune shift with amplitude, which can be used to improve the solution of harmonic sextupoles, and thus obtain a large dynamic aperture. The second one is the tune diffusion rate, which can be used to select a quiet tune. Application of these ideas is carried out in the storage ring of the Shanghai Synchrotron Radiation Facility (SSRF), and the detailed processes, as well as better solutions, are presented in this paper. Discussions about the nonlinear behaviors of off-momentum particles are also presented.

Key words SSRF storage ring, nonlinear optimization, dynamic aperture, FMA

PACS 29.20.dk, 41.85.-p, 42.65.-k

1 Introduction

The modern synchrotron radiation storage rings use very strong quadrupoles to achieve low emittance, but unfortunately they suffer from large natural chromaticities, which must be compensated by strong sextupole fields in order to suppress the head-tail instability[1]. Corresponding nonlinearity of the sextupoles drastically limits dynamic acceptances of the lattice. Commonly, harmonic sextupoles are introduced in the lattice to optimize the nonlinearity, and thus enlarge the dynamic acceptances to reach high injection efficiency and long beam lifetime[2].

Many methods, including numerical approaches and analytical ones, can be applied in the nonlinear optimization of the storage ring. There are three examples presented here in brief. The first one is scanning of the harmonic sextupole integral strengths, and it can be used in a simple lattice with one or two harmonic sextupole families, such as ASP[3] and ELETTRA[4]. The second one is a step-by-step approach, in which the best pair of focusing and defocusing sextupoles is used to compensate small chromaticities released by chromatic sextupoles and enlarge the dynamic aperture step-by-step. It has been applied in the SSRF storage ring, and acceptable solutions were derived[5]. The third one is an analytic approach based on the perturbation theory. In this method, the Hamiltonian of the particle, impacted by the quadrupoles and the sextupoles, is decomposed to a series of driving terms of different orders. Suppression of the most dangerous terms is expected to result in large dynamic acceptances. At present, it is extensively applied in the storage rings of the modern third generation light source, such as DIAMOND[6] and NSLS-II[7].

Although these methods can be used to obtain large dynamic acceptance for a given lattice and optical functions, details in the dynamic acceptance and mechanism of the beam loss are ambiguous. The Frequency Map Analysis (FMA) builds one-to-one maps between orbits and frequencies[8]. Tune shifts with amplitudes and tune diffusions with times are used to reveal the fine structures of the nonlinear resonances.

Received 11 April 2008
* Supported by SSRF Project
1) E-mail: tianshunqiang@sinap.ac.cn
2) E-mail: liugm@sinap.ac.cn

With the detailed information, it is easy to comprehend the mechanism of the beam loss. After the first application in ALS by J. Laskar in 1990s'[9], many circular accelerators all over the world applied FMA to investigate the nonlinear behaviors of the surviving particle and tend to re-optimize the nonlinearity of the ring. One can find the details in Refs. [10—15].

FMA is usually regarded as a qualitative analytic tool. This fact leads to redoing the optimization algorithm more frequently, and sometimes, it is still difficult to obtain a good solution. In this paper, we particularly discuss two benefits of FMA, and use them to improve step-by-step the optimum solution resulting from the optimization algorithm, without frequently revisiting the algorithm. The first benefit is the tune shifts with amplitudes reveled by FMA. It can be used to qualitatively investigate effects of the tune shifts, including not only the linear tune shifts but also the high order tune shifts. If there are two solutions with different tune shifts (opposite direction), we can obtain an improved one with the tradeoff between them. The second benefit is the tune scanning carried out by the footprint of the tune shift with different diffusion, and it can be used to select a quiet tune avoiding dangerous nonlinear resonances. With the two stratagems, we optimize the nonlinearity of the SSRF storage ring. Optimization process as well as optimum solution are presented in details in following sections.

2 Descriptions of frequency map analysis

Considering an integrable system with n degrees of freedom, the motion in phase space takes place on tori, which are described at constant frequency $\nu_j(\boldsymbol{I})$. If the system is non-degenerate, the frequency map[8]

$$\boldsymbol{I} \rightarrow \boldsymbol{\nu} \tag{1}$$

is a one-to-one smooth map on its image, and the tori are as well described by the action variables ($\boldsymbol{I}$) or by the frequency vector ($\boldsymbol{\nu}$). For a non-degenerate system with perturbation, KAM theorem[16] still asserts that for sufficiently small values of ε, there exists a Cantor set of values of ν, satisfying a Diophantine condition, for which the perturbed system still possesses smooth invariant tori with linear flow (the KAM tori).

In a storage ring, the motions of the particles are perturbed by sextupoles. And thus, in the phase space, the smooth invariant tori construct the dynamic aperture. And the out of the dynamic aperture is chaotic, where the particles will lose. In the dynamic aperture, there are still some broken tori, which are random layers, and characterize nonlinear resonances.

If we track some test surviving particles with different initial conditions, and the variables are recorded for each turn for the time span T (or the turn number N), we can search for a quasi-periodic approximation of particle motion of the form, as formula (2), by using a numerical algorithm based on a refined Fourier technique (numerical analysis of the fundamental frequency)[17], which provides a tune accuracy of $1/T^3$ (or $1/N^3$).

$$z_w(t) = a_w \mathrm{e}^{\mathrm{i}\nu_w t} + \sum_{k=1}^{N} a_k \mathrm{e}^{\mathrm{i}(m_k,\boldsymbol{\nu})t} , \tag{2}$$

where $w = x, y$, $\boldsymbol{\nu}$=(ν_x, ν_y, 1) is the fundamental frequency vector, $m_k = (m_{xk}, m_{yk}, m_{3k})$ is a multi-index and the complex amplitude α_k is ordered by decreasing magnitudes. If the motion of the particle is close to integrable, its fundamental frequency vector can be accurately identified and with small diffusion, and this indicates a stable motion. If the motion of the particle is in the random layer or on the resonance, the calculated frequency vector has large diffusion, and this indicates an instable motion.

In this paper, each particle is tracked over 1000 turns and for the surviving particle the transverse tunes ($\nu_x^{(1)}$, $\nu_y^{(1)}$) and ($\nu_x^{(2)}$, $\nu_y^{(2)}$) are computed with FMA over two consecutive samples of 500 turns. The diffusion rate D is then calculated as

$$D = \lg\sqrt{\left(\nu_x^{(1)} - \nu_x^{(2)}\right)^2 + \left(\nu_y^{(1)} - \nu_y^{(2)}\right)^2} , \tag{3}$$

and is used as a stability index. The diffusion rate is coded by grey shadings from white for very stable orbits to black for unstable or chaotic ones.

With the footprint and the tune diffusion rate revealed by FMA, it is easy to understand the mechanism of beam loss, and the nonlinear resonances can be easily characterized qualitatively in the aspects of strengths and stopbands. Commonly, together with the reduction of nonlinear driving terms, the minimization of tune shifts with amplitude is an important issue for nonlinear optimization. With nonlinear perturbation, the high order tune shifts with amplitude are remarkable to affect the global dynamics of the lattice. The footprint of the frequency map is available to investigate the high order tune shifts with amplitude and improve the nonlinear optimum solution. Moreover, a quiet tune can be found by the tune scanning carried out by footprint of the tune shift with different diffusion. More details are presented in Section 4.

3 Descriptions of the nonlinear optimization algorithm

In this paper, we achieve the first solutions with an analytic optimization algorithm based on the perturbation theory, and then improve these solutions with the information revealed by FMA. This analytic algorithm decomposes the Hamiltonian of the particle, impacted by the quadrupoles and the sextupoles, to a series of driving terms of different orders, and supposes these terms generate relevant resonances that degrade the lattice acceptances. The lower order terms are usually considered to be the most dangerous ones. A penalty function consisting of low order terms is converged to a valley that is expected to provide large dynamic acceptances[18]. For a convenient condition and fast calculating speed, the geometric terms of the first order and linear tune shift terms of the second order are introduced in our employed penalty function. It is envisaged that the solution of the sextupole depend strongly on the weight setting for the driving terms and starting values for the sextupole strengths.

There are several facts that should be noted. The first one is that the solution resulting from this analytic optimization algorithm can obtain small considered driving terms, which is necessary to better nonlinear behaviors of the particles. The second one is that the higher order terms, which haven't considered in the algorithm, may have strong effects on the nonlinear behaviors, especially the high order tune shift terms. The third one is that FMA can reveal more information about the nonlinear behaviors, especially the tune shift with amplitude, containing the high order tune shift, and it can be applied to improve the solution of the algorithm.

4 Nonlinear optimizations in the SSRF storage ring

4.1 SSRF storage ring

The accelerators of the SSRF project[19, 20] were installed in ten months from November 2006, and were successfully tested and commissioned in the past several months. The storage ring consisting of 20 Double Bend Achromatic (DBA) cells with four super-periods is designed with low emittance of 3.9 nm·rad to provide high photon brightness. Each super-period contains three standard cells and two matching cells. There are 200 quadrupoles classed in ten families and 140 sextupoles classed in 8 families in the storage ring. Each quadrupole is excited by a separate power supply, for restoring periods of the optical functions with presence of magnetic errors and insertion devices. Each family of the sextupoles is excited by one power supply, in which $S1$, $S2$, $\cdots$, and $S6$ are the harmonic sextupoles. The main parameters of the storage ring are summarized in Table 1. Fig. 1 depicts the lattice layout and the typical linear optical functions of one super-period[21].

Table 1. Main parameters of the SSRF storage ring.

parameters	value
energy/GeV	3.5
circumference/m	432
cell	20(DBA)
super-period	4
tune Q_x, Q_y	22.22, 11.32
β_x, β_y, η_x/m in the centers of	10, 6.0, 0.15
straight sections	3.6, 2.5, 0.10
natural emittance/(nm·rad)	3.92
natural chromaticity ξ_x, ξ_y	-55.64, -17.94
momentum compactor	4.2118×10^{-4}
damping partitions J_x, J_y, J_s	0.9968, 1, 2.0032
damping times τ_x, τ_y, τ_s/ms	6.97, 6.95, 3.47
natural energy spread/rms	9.8958×10^{-4}

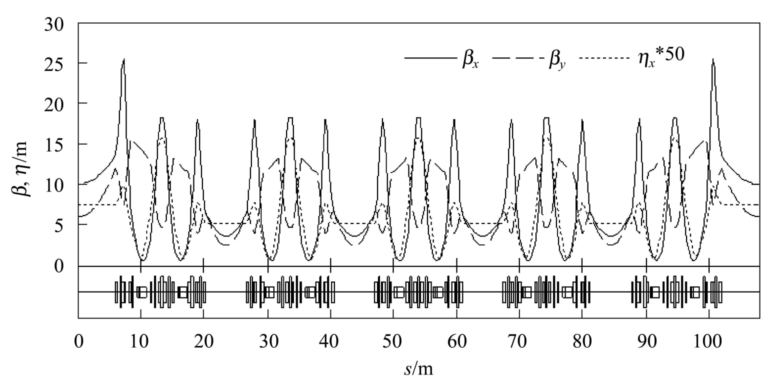

Fig. 1. Typical linear functions of one super-period in the SSRF storage ring.

4.2 Solutions resulting from the analytic optimization algorithm

With the application of the analytic optimization algorithm, many solutions of the sextupoles can be obtained. Detailed information inside the dynamic aperture can be revealed by FMA, and then, we can recognize which resonance degrades the dynamic aperture, and get the knowledge of the reason for small dynamic aperture. Two solutions with different footprints of the tune shift with amplitude are quoted in Fig. 2 and Table 2. From Fig. 2, it is envisaged that the main reason of a small dynamic aperture is not some single resonance, but may be integrated effects of a series of resonances and the large tune shift. Except for the nonlinear resonances and small dynamic aperture, one can find that the two frequency maps have different directions. It has been realized that big dynamic aperture can be achieved by small geometric terms and tune shift terms. With the analytic optimization algorithm, small low-order geometric terms and linear tune shift terms can be reached by a fast convergent method, so the main part of the large tune shift is the high order tune shift terms. A small tune shift can be reached by a tradeoff between the two solutions without frequently revisiting the optimization algorithm or introducing high order tune shift term to the penalty function.

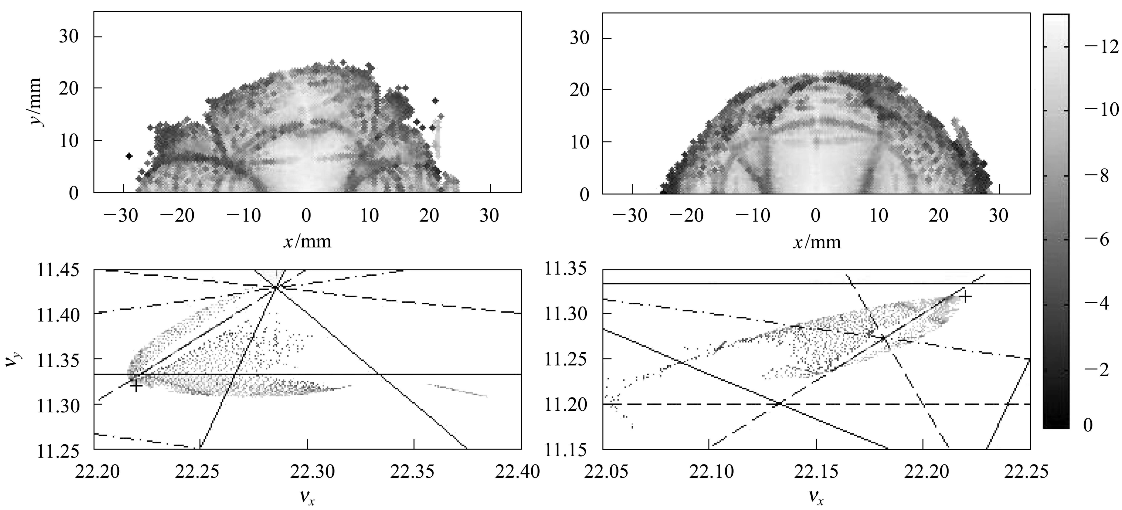

Fig. 2. Frequency maps and dynamic apertures of the two solutions, where the tunes are 22.22, 11.32.

Table 2. Two solutions resulting from the optimization algorithm.

sextu. fam.	effect. length/m	solution a (1/m^2)	solution b (1/m^2)
S1	0.213	1.5722	1.5243
S2	0.253	−3.7515	−2.8533
S3	0.213	2.7755	2.6646
S4	0.253	−2.8616	−2.9244
S5	0.213	4.3110	3.4548
S6	0.253	−4.9822	−4.5561
SF	0.253	3.2618	3.5497
SD	0.213	−2.3042	−2.4488

4.3 The combined solutions

Table 3 lists the integral strengths of the harmonic sextupoles of the tradeoff between the solution (a) and (b). It is done by a simple linear addition, i. e. $1/3\times a + 2/3\times b$. The chromaticities are corrected to zero for both transverse planes. The dynamic aperture and the frequency map are showed in Fig. 3.

Table 3. Solution c combined with a and b.

sextu. fam.	integral strength (1/m^2)
S1, S3, S5	1.5403, 2.7016, 3.7402
S2, S4, S6	−3.1527, −2.9035, −4.6982

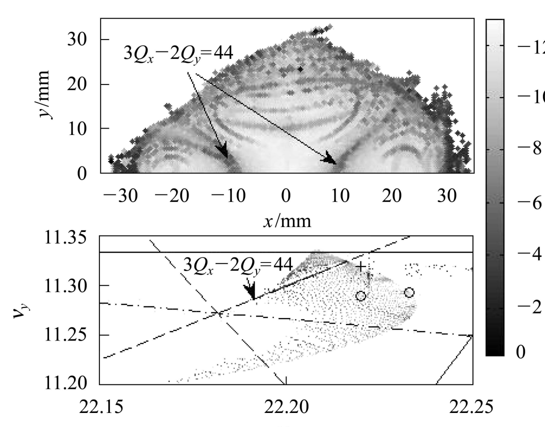

Fig. 3. Frequency map and dynamic aperture of the combined solution at the tune of 22.22, 11.32.

With this combined solution, a small tune shift map is obtained, and thus a larger dynamic aperture is reached.

Table 4. Values of the driving terms of the three solutions.

term	effect	No HS	a	b	c
$\|h_{10110}\|$	ν_x	31.040	5.1533	2.5557	3.4209
$\|h_{10200}\|$	$\nu_x+2\nu_y$	5.8363	5.6772	2.4361	3.5162
$\|h_{10020}\|$	$\nu_x-2\nu_y$	113.35	4.8316	4.7616	4.7817
$\|h_{21000}\|$	ν_x	48.595	7.1529	2.5877	0.6612
$\|h_{30000}\|$	$3\nu_x$	5.4816	1.8778	1.3743	1.5421
$\|h_{20001}\|$	$2\nu_x\|_{\delta\neq0}$	11.453	10.944	11.743	11.477
$\|h_{00201}\|$	$2\nu_y\|_{\delta\neq0}$	0.8994	1.1018	1.6411	1.4614
$\|h_{22000}\|$	$\partial\nu_x/\partial J_x$	171940	1078.9	301.81	1466.9
$\|h_{11110}\|$	$\partial\nu_{x,y}/\partial J_{y,x}$	135120	2728.7	272.61	1483.8
$\|h_{00220}\|$	$\partial\nu_y/\partial J_y$	472.33	53.822	1040.1	682.10

Table 4 lists the low order driving terms of the three solutions and the case without harmonic compensation. When there is no harmonic sextupole, the driving term is very large, especially the linear tune shift term, and it is impossible to get an ample dynamic aperture. The analytic optimization algorithm can result in some solutions with low driving terms, however, it is difficult to obtain an acceptable dynamic aperture without frequently revisiting the algorithm or attempting a variety of weight settings of the driving terms and starting values of the harmonic sextupoles. With the application of FMA, an improved solution resulting in large dynamic aperture can be achieved by a simple tradeoff between two solutions with opposite tune shifts. The geometric terms are not enlarged. Although some terms of the linear tune shift of the solution (a) and (b) are smaller than the ones of solution (c), it is expected that the solution (c) can suppress the high order tune shift terms more sufficiently.

4.4 Choosing a quiet tune with FMA

As the former discussions, a better solution of the harmonic sextupoles is reached, but for the tunes of 22.22, 11.32, there is still a serious nonlinear resonance ($3Q_x-2Q_y=44$) in the dynamic aperture. As a structure resonance, it may lead the injected beam to loss, and thus reduce the injection efficiency. It is difficult to control the tune shift to keep away from this resonance by readjusting the strengths of the harmonic sextupoles without reduction of the dynamic aperture, so new tune should be chose in order to get a better frequency map. In a small tune zone, the FMA is a good method of tune scan by using the diffusion rate. We select two tunes close to the referent one ($Q_x,\ Q_y=22.22,\ 11.32$), and avoid new serious nonlinear resonance affecting the injection by considering elaborately the tune diffusion rate shown in the bottom figure of Fig. 3, where the two new tunes are denoted by 'o'. The dynamic apertures and frequency maps of the two new tunes are showed in Fig. 4, in which the left two figures are for the tune of 22.22, 11.29, and the right two figures are for the tune of 22.233, 11.294. The most remarkable nonlinear resonance is $2Q_x+2Q_y=67$ in both frequency maps. The inter parts of the dynamic apertures are resonance-free, and this is helpful to increase the injection efficiency.

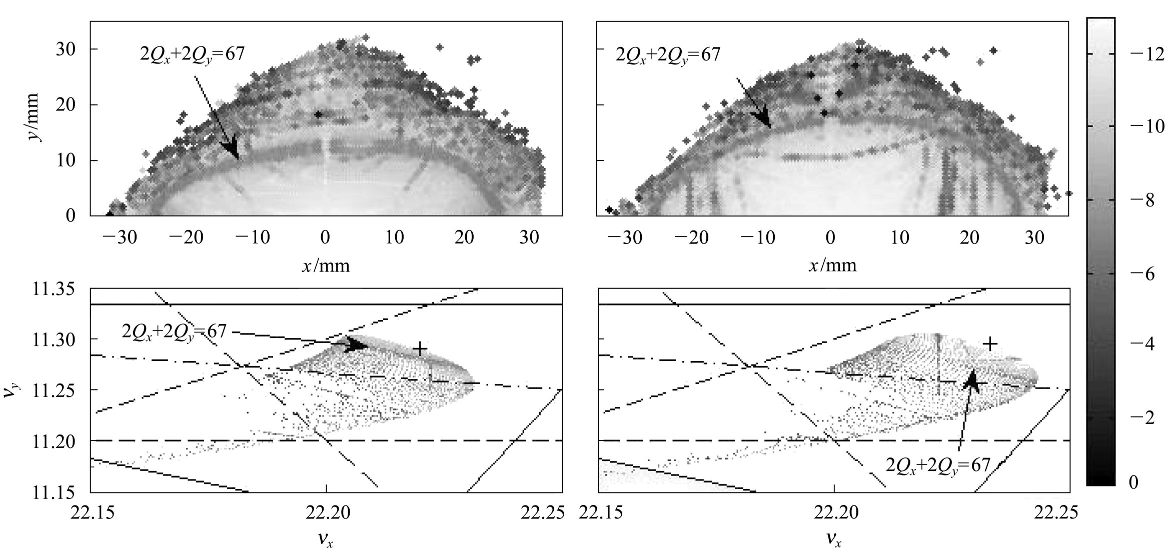

Fig. 4. Frequency maps and dynamic apertures at the tunes of 22.22, 11.29 (the left two figures) and 22.233, 11.294 (the right two figures).

Table 5. The driving term values of 22.22, 11.29 and 22.233, 11.294, as well as the cases without harmonic sextupoles.

term	without HS 22.22,11.29	solution c 22.22,11.29	without HS 22.233,11.294	solution c 22.233,11.294
$\lvert h_{10110}\rvert$	31.093	3.6365	32.479	3.4880
$\lvert h_{10200}\rvert$	8.6553	5.2876	7.7165	4.5917
$\lvert h_{10020}\rvert$	125.12	5.1990	126.49	5.2393
$\lvert h_{21000}\rvert$	48.533	0.6427	50.918	0.3449
$\lvert h_{30000}\rvert$	5.4683	1.5424	4.8889	1.4827
$\lvert h_{20001}\rvert$	11.449	11.472	11.245	11.278
$\lvert h_{00201}\rvert$	1.0654	1.6802	1.0447	1.6545
$\lvert h_{22000}\rvert$	171630	1414.2	173060	1442.3
$\lvert h_{11110}\rvert$	144440	1340.5	146170	1325.9
$\lvert h_{00220}\rvert$	4900.7	654.35	5542.5	688.98

Table 5 lists the values of the first order driving terms and linear tune shift terms, including the two new tunes and the cases without harmonic sextupole compensation. All the considered terms have been suppressed sufficiently in both two tunes with the same solution of harmonic sextupoles.

5 Investigation of the nonlinear behaviors of off-momentum particles

Figure 5 depicts the dynamic apertures of the horizontal plane and the longitudinal plane, in which the left two figures are for the tune of 22.22, 11.29, and the right two figures are for the tune of 22.233, 11.294. We don't consider the radiation and the energy compensation of cavity here. When there is no transverse amplitude, the first resonance of off-momentum particle occurs at $\delta = -3\%$ and 3% for the tune of 22.22, 11.29, and at -5% and 4.5% for the tune of 22.233, 11.294. Fig. 6 shows the working points as a function of momentum deviation, where the difference resonance $Q_x - Q_y = 11$ occurs at about 4.5% of the momentum deviation for both the two tunes. With the large resonance-free momentum acceptances, it is easy to increase the beam lifetime.

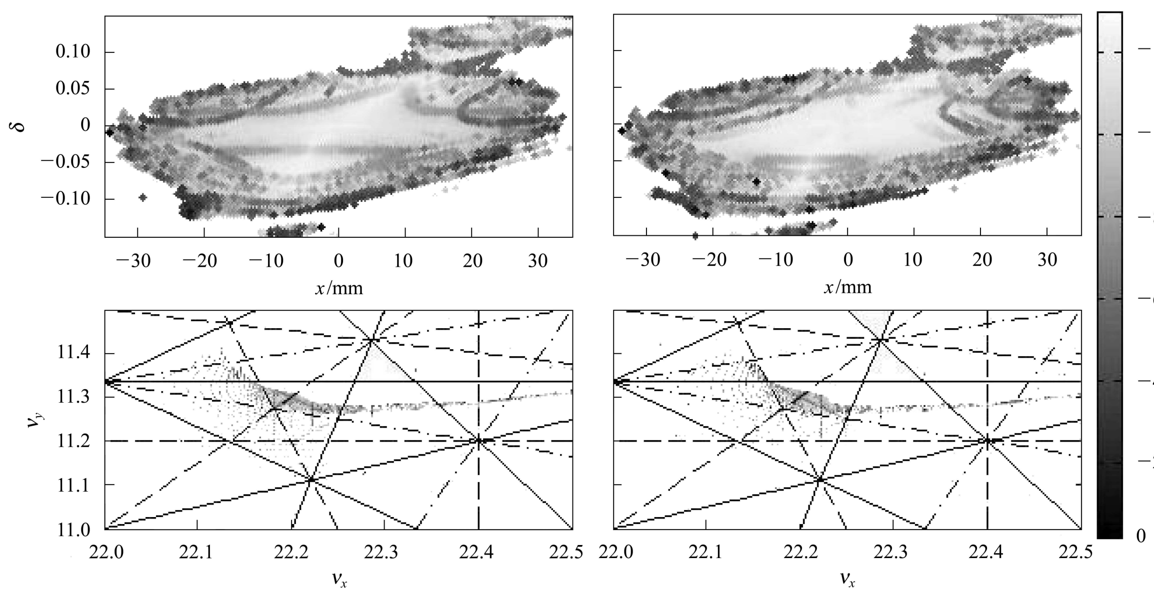

Fig. 5. Frequency map with momentum deviations, the left two figures are for 22.22, 11.29, and the right two figures are for 22.233, 11.294.

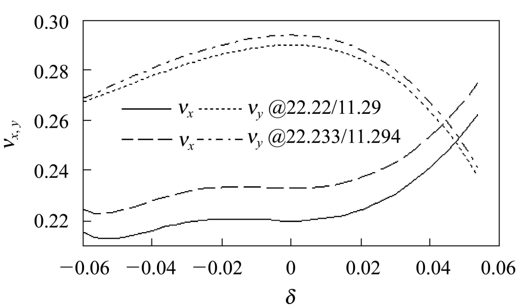

Fig. 6. The working points as a function of momentum deviation.

Asymmetry of the β function is the main reason for asymmetry of the dynamic aperture with respect to the momentum deviation[22], and it strongly depends on the correctional effect of the sextupoles[23]. For a better nonlinear solution of the sextupoles, the β function should vary smoothly with momentum deviation, and avoid large β-beating, in order that symmetric dynamic aperture with respect to momentum deviation can be achieved. Fig. 7 plots β as a function of momentum deviation. In fact, the β functions of two tunes have the same variation. These results are acceptable, because the square roots of the β functions have small range, which is from 2.8 for momentum deviation of 3% to 3.5 for momentum deviation of -3% in the horizontal plane, and from 2.4 to 2.6 in the vertical plane approximately. The common optical mode of the SSRF storage ring has little dispersion in the long straight section (0.15 m),

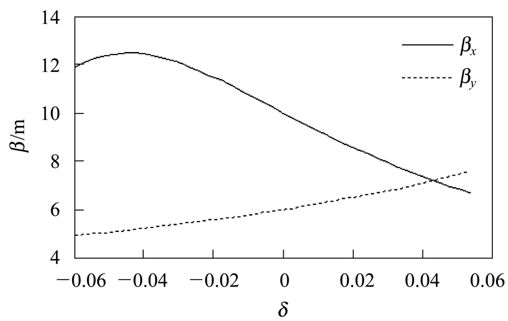

Fig. 7. β functions as a function of momentum deviation.

so the centre of the off-momentum dynamic aperture moves from -4.5 mm for -3% momentum deviation to 4.5 for 3% momentum deviation in the horizontal plane. It is even impossible to get a symmetric dynamic aperture with a consist β-function with momentum deviation.

Figure 8 depicts the dynamic apertures of off- and on-momentum particles for the two tunes, which are obtained by tracking for 1000 turns. The symmetries are good, and the acceptances are ample to get high injection and long beam lifetime. The size of the physical chamber in the SSRF storage ring is 32 mm in the horizontal plane, and 16 mm in the vertical plane without insertion device. The max β-function along the ring is about 25 m in the horizontal plane and 15 m in the vertical plane, shown as Fig. 1, so the max aperture in the centre of the long straight section, scraped by the vessel, is about 20, 10 mm (horizontal, vertical), which are smaller than the dynamic apertures resulting from the optimum solutions.

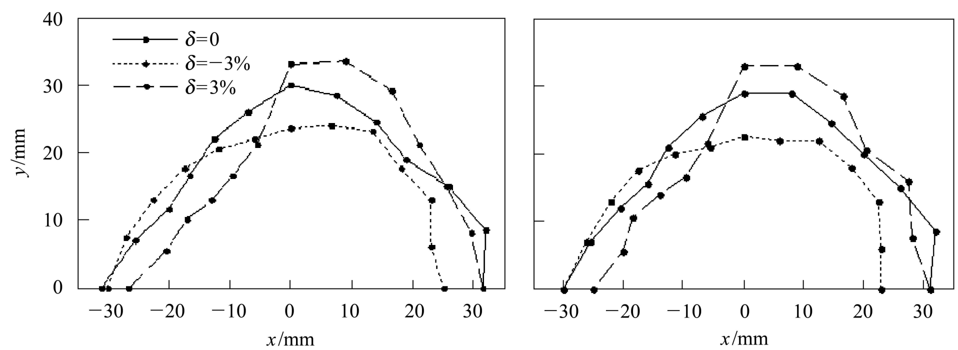

Fig. 8. Dynamic apertures of off- and on-momentum particles, tracking for 1000 turns, the left figure is for $Q_x, Q_y = 22.22$, 11.29, and the right one is for $Q_x, Q_y = 22.233$, 11.294.

6 Conclusions

With the application of FMA to the SSRF storage ring, the fine structure of the nonlinear resonance is revealed, and it shows that the restriction of dynamic aperture is not some single resonance but the integrated effect of nonlinear driving force in the modern third generation light source. With the information about the tune shift of FMA, nonlinear optimum solutions resulting from optimization algorithm have been improved. Some quiet tunes close to the referent ones can be found with the tune scanning carried out by frequency maps. The two benefits of FMA, i. e. tune shift with amplitude and tune diffusion rate, are applied to the nonlinear optimization process, and better solutions are obtained without ambiguously finding a better tune in the tune diagram or frequently revisiting the optimization algorithm. It is claimed that this optimization method or process can be applied in the other third generation light source storage ring, and can reach large dynamic acceptance, which avoids serious nonlinear resonance.

References

1 Sands M. SLAC TN-69-8, Stanford, 1969
2 Smith S L. Proceedings of the European Particle Accelerator Conference. France: Paris, 2002. 44—48
3 Tan Y R E. Proceedings of the Particle Accelerator Conference. Knoxville, USA: Tennessee, 2005. 407—409
4 Tosi L, Bocchetta C J, Iazzourene F et al. Proceedings of the European Particle Accelerator Conference. England: London, 1994. 1006—1008
5 TIAN Shun-Qiang, HOU Jie, CHEN Guang-Ling, LIU Gui-Min. Chinese Physics C (HEP & NP), 2008, **32**: 661—664
6 Owen H, Jones J, Smith S. Proceedings of the European Particle Accelerator Conference. France: Paris, 2002. 751—753
7 Bengtsson J. Proceedings of the European Particle Accelerator Conference. Scotland: Edinburgh, 2006. 3478—3480
8 Laskar J. Proceedings of the Particle Accelerator Conference. Portland, USA: Oregon, 2003. 378—382
9 Dumas H S, Laskar J. Phys. Rev. Lett., 1993, **70**: 2975
10 Sterier C, Robin D, Nadolski L et al. Phys. Rev. E, 2002, **65**: 056506
11 Turchetti G, Bazzani A, Bergamini F et al. Nucl. Instrum. Methods A, 2001, **464**: 551
12 Robin D, Krupnick J, Schlueter R et al. Nucl. Instrum. Methods A, 2005, **538**: 65
13 Mitri S Di, LIU G M, Tosi L. Proceedings of the European Particle Accelerator Conference. Switzerland: Lucerne, 2004. 2062—2064
14 Kuske P. Proceedings of the Particle Accelerator Conference. Knoxville, USA: Tennessee, 2005. 266—268
15 JIAO Y, FANG S X, QIN Q et al. Nucl. Instrum. Methods A, 2006, **566**: 270
16 Arbold V I, Kozlov V V, Neishtadt A I. Mathematical Aspects of Classical and Celestial Mechanics: Dyn. Systems III. New York: Springer, 1988
17 Nadolski L, Laskar J. Phys. Rev. ST, 2003, **6**: 114801
18 Bengtsson J. The Sextupole Scheme for the Swiss Light Source, SLS Note 9/97
19 ZHAO Z T, XU H J. Proceedings of the European Particle Accelerator Conference. Switzerland: Lucerne, 2004. 2368—2370
20 XU H J, ZHAO Z T. Nuclear Science and Technique, 2008, **19**: 1—6
21 LIU G M, DAI Z M, LI H H et al. HEP & NP, 2006, **30**(Supp. Ⅰ): 144 (in Chinese)
22 FANG Shou-Xian, QIN Qing. HEP & NP, 2006, **30**(9): 880 (in Chinese)
23 TIAN Shun-Qiang, HOU Jie, CHEN Guang-Ling, LIU Gui-Min. Chinese Physics C (HEP & NP), 2008, **32**: 576—579